CHARACTERISTICS OF EARTHQUAKE DISPLACEMENT MOTIONS WITH EMPHASIS ON THEIR LONG-PERIOD COMPONENTS

by

Nobuhiko SATO[I], Keizaburo KUBO[II], and Tsuneo KATAYAMA[III]

SYNOPSIS

The characteristics of velocity and displacement motions derived from the accelerograms recorded at four sites during the main shock and the largest aftershock of the 1968 Tokachi-Oki earthquake are discussed. The effects of earthquake magnitude and the depth to the seismic bedrock are examined on the peak and the r.m.s. amplitudes of velocity and displacement. The properties of displacement motions in the frequency domain are analyzed by using the output from a digital bandpass filter.

INTRODUCTION

Due to the recent advancement in design and construction technology, modern structures are becoming increasingly taller, longer and larger than their conventional counterparts. Consequently, natural periods of modern structures tend to become longer, whereby dynamic effects due to long-period components of earthquake ground motions are drawing seismic engineers' attention. Though strong earthquake motions are usually recorded by accelerographs, effects of long-period components may be better understood by displacement of ground motions. Ordinary accelerograms show very small acceleration amplitudes for long-period waves, but their effects on long-period structures are often greater than those of short-period and large-amplitude acceleration waves. It is also said that sloshing of liquid in large storage tanks are closely related to the displacement amplitudes of earthquake ground motions (1).

By considering the importance of displacement amplitudes of earthquake ground motions, it is highly desirable to define their velocity and displacement wave forms in addition to the conventional accelerograms. There have been a number of methods proposed for transforming an acceleration record into a displacement record, and a large number of the U.S. accelerograms were systematically transformed into displacement waves bt the researchers in the California Institute of Technology by using a method developed there. It is generally impossible to obtain reliable displacement wave forms for very low frequency components from recorded accelerations. However, such transformation in the frequency range of engineering interest still seems to be one of the important problems for the future advancement of earthquake engineering.

EARTHQUAKE RECORDS AND METHOD OF ANALYSIS

The earthquake used for the analysis reported in this paper are the main shock (M=7.9) and the largest aftershock (M=7.5) of the 1968 Tokachi-Oki earthquake. Acceleration wave forms were obtained by SMAC-B2 type strong-motion seismographs installed on the ground surface at Aomori, Hachinohe, Muroran and Miyako (see Fig.1). For Hachinohe, the record of the aftershock was not available. Some of the parameters of the earthquakes and the epicentral distances for the four observation stations are summarized in Table 1. The digitized values of accelerograms were taken from Ref.(2) and were used at a time increment of 0.02sec. The length of an accelerogram analyzed was 30 seconds, which included the largest

[I]Research Assistant, [II]Professor and [III]Associate Professor of the Institute of Industrial Science, University of Tokyo.

acceleration, except for the aftershock record at Miyako for which the length was 25 seconds. It should be noted that the recorded accelerograms did not have a common time signal, hence there was no time correspondence among the records obtained at the four sites.

The method used here for transforming an acceleration record into a displacement wave form is discussed elsewhere in detail (5). The corrections of acceleration are made by introducing linear base-line correction and amplitude correction not exceeding a certain specified value, Δ. These correction terms are so determined as to minimize the value of the r.m.s. amplitude of velocity. It was demonstrated experimentally that the optimum value of Δ to be used for amplitude correction was 1% of the maximum acceleration amplitude for the records obtained by the SMAC-B2 type seismograph.

Original accelerograms are obtained in the NS and the EW direction, from which acceleration records were synthesized at each site in the radial and the tangential direction with respect to the instrumental epicenter. The physical meaning of these two directions is not clear because energy release during an earthquake takes place over a large area and the instrumental epicenter alone does not furnish any information about the configuration and the motion of the causative fault. In all, velocity and displacement curves were calculated for the four directions (NS, EW, Radial and Tangential) at each site for each earthquake.

Displacement curves were analyzed in the frequency domain by using a digital nonrecursive bandpass filter with the even weighting function. The width of the bandpass filter was set as 20% of the central frequency, 10% each on the both sides of the central frequency of the filter. The power spectral density function in this study is defined as the mean square of output amplitudes divided by the width of the filter.

Fig.2 shows the boring logs and the variations of standard penetration N-values at the four observation sites. As seen from the N-value variations in Fig.2, the thickness of soft surface layers is the largest at Aomori and the smallest at Miyako. According to Tsuchida and Uwabe (3), the fundamental periods calculated by the theory of multiple-reflection of shear waves were 0.77 seconds at Aomori, 0.24 seconds at Hachinohe, 0.23 seconds at Muroran and 0.20 seconds at Miyako. However, even from the analysis of accelerograms, much longer predominant periods were observed during the 1968 Tokachi-Oki earthquake for Aomori (about 3 seconds) and for Hachinohe (about 2.5 seconds). It is reported (4) that such long predominant periods may be attributable to the thickness of surface layers relative to the so-called seismic bedrock. The depth to the seismic bedrock is estimated (4) as about 700m at the Aomori site, about 400m at the Hachinohe site, whereas the bedrock is found only at a depth of approximately 10m at the Miyako site. For the Muroran site, the depth to the bedrock is not known.

CHARACTERISTICS OF DISPLACEMENT MOTIONS

The maximum and the r.m.s. amplitudes in the four directions analyzed are summarized in Table 1. Since the reliability of integrated displacement motions decreases for the lower frequency components, displacement amplitudes only for the components having frequencies greater than 0.1Hz are also listed in parentheses. In the following, the maximum of displacement amplitudes in the four directions with frequency components greater than 0.1Hz (values in parentheses) will be discussed unless otherwise stated.

It is seen from Table 1 that the epicentral distances of the four observation sites vary approximately from 200km to 300km. For the main shock with magnitude 7.9, the maximum velocity amplitude is roughly 40 kine at Aomori and Hachinohe, 30 kine at Muroran and 6 kine at Miyako. The maximum displacement amplitudes is about 20cm at Aomori, 10cm at Hachinohe and Muroran, and 1cm at Miyako. It is observed from Fig.1 that the directions from the epicenter to Aomori and to Hachinohe are much the same, while the epicentral distance to Aomori (243km) is about 30% greater than that to Hachinohe (188km). However, the maximum displacement at Aomori is nearly twice larger than that at Hachinohe. This may be accounted for by the difference in the depths to the seismic bedrock at these two sites. As was mentioned previously, the depth to the seismic bedrock at Aomori is estimated as about 700m while that at Hachinohe as 400m. The small value of the maximum displacement (about 1cm) at Miyako could be also explained by the fact that the seismic bedrock lies at a very shallow depth there. Nothing definite can be said about the maximum displacement of about 10cm at Muroran since the depth to the bedrock is not available. It may be inferred, however, that the depth at Muroran is larger than that at Miyako even though the soil profiles shown in Fig.2 at these two sites look similar. An exceptional value is observed at Miyako during the aftershock. The maximum displacement of about 1cm for the frequency components greater than 0.1Hz is almost the same as that obtained for the main shock, whereas the displacement amplitudes during the aftershock at Aomori and Muroran are much smaller than those during the main shock. From the data of Aomori and Muroran, an interesting tendency is found for the effect of earthquake magnitude on the amplitudes of ground motions. Table 2 summarized the ratios between the r.m.s. amplitude of the aftershock and that of the main shock. The ratios are the highest for acceleration amplitude and the lowest for displacement amplitude. This indicates that the effect of earthquake magnitude on ground motion amplitude is generally more pronounced in displacement than in acceleration. This tendency agrees with the results of the regression analysis made for the U.S. strong motion records (6).

It is interesting to examine the ratios of the peak amplitude and the r.m.s. amplitude from the data shown in Table 1. The average ratio was found to be approximately 4 for acceleration and velocity motions, and 3 for displacement motion. Therefore, the peak amplitude of ground motions during strong earthquakes is generally 3 to 4 times greater than their r.m.s. amplitude.

The calculated displacement curves for the main shock in the radial and the tangential direction are shown in Fig.3. It is seen from this figure that the displacement motions in the radial direction seem to contain more longer-period components than those in the tangential direction. This can be confirmed by examining the ratios of the r.m.s. amplitude of the greater-than-0.1Hz components (values in parentheses) and that of the displacement motions including the less-than-0.1Hz components shown in Table 1. These ratios are roughly 0.4 to 0.7 in the radial direction and 0.7 to 1.0 in the tangential direction.

Calculated displacement curves were analyzed in the frequency domain by using the output from a digital bandpass filter. Fig.4 shows the distribution of the maximum amplitudes of filtered displacement curves. Note that the width of the digital filter is 20% of the center frequency and that the maximum filtered displacements are plotted at the locations of the corresponding center frequencies. The power spectral density functions as defined previously are shown in Fig.5 for the calculated displacement motions. The vertical axis of Fig.4 is in the linear scale while that of Fig.5 is in the logarithmic scale.

From Figs.4 and 5, predominant peaks are apparent in the tangential direction at Aomori during both earthquakes and in the radial and tangential directions at Hachinohe during the main shock. For the motions at Muroran and Miyako, it is difficult to observe distinct peaks regardless of direction or earthquake. The general tendency in all the cases examined is the increase of power spectral density with the decrease in frequency. In most of the cases, the power spectral density at 0.1Hz is about 100 times greater than that at 1Hz. The overall similarity of the frequency characteristics of the displacement motions at Muroran and Miyako is evident. However, as mentioned previously, there is a large difference between the displacement amplitudes at these sites. It is not attempted at present to explain the reason for these apparently contradictory tendencies. By examining the corresponding frequencies of the predominant peaks in the tangential motion at Aomori, it is seen that the peak at 0.32Hz during the main shock shifted to that at 0.45Hz during the aftershock. Though not so conclusive, a similar trend is also found in the radial motion at Aomori.

CONCLUDING REMARKS

The following concluding remarks may be made from the studies reported in this paper, though much more information is required before any reliable and useful characteristics of long-period displacement motions can be established.

(1) Displacement and velocity amplitudes of strong seismic ground motions on the surface of ground seem to be related to the depth to the seismic bedrock, which is often located several hundreds of meters below the ground surface. (2) The effect of earthquake magnitude on amplitude is the greatest in displacement motion and the least in acceleration motion. (3) Displacement ground motion in the radial direction seems to contain more components with frequencies less than 0.1Hz than that in the tangential direction. (4) Displacement ground motions at certain sites exhibit predominant frequencies within the range between 0.1 and 1Hz in certain directions while no such tendency is found in some other cases.

REFERENCES

(1) S.Yamamoto and N.Shimizu; "Effects of Earthquake Motions with Long-Period Components for Long-Period Structures", Kenchiku-Gijutsu, June, 1974. (2) H.Tsuchida, E.Kurata and K.Sudo; "Strong-Motion Earthquake Records of the 1968 Tokachi-Oki Earthquake and Its Aftershocks", Technical Note of the Port and Harbour Research Institute, No.80, June, 1969. (3) H.Tsuchida and T.Uwabe; "Characteristics of Base-Rock Motions Calculated from Strong-Motion Accelerograms at Ground Surface", Report of the Port and Harbour Research Institute, Vol.11, No.4, Dec., 1972. (4) Y.Ohta, K.Kudo and others; "Applications of the Microtremors in Semi-Long-Period Range to Earthquake Engineering, Part 4, Comparisons of Strong-Motion Accelerograms Recorded by SMAC-B2 during the 1968 Tokachi-Oki Earthquake", Preprint of the Spring Meeting of the Seismological Society of Japan, May, 1976. (5) K.Kubo and N.Sato; "A Method for Obtaining Reliable Displacement Curves from Recorded Earthquake Motions", Proceedings of the Fourth Japan Earthquake Engineering Symposium, Nov., 1975. (6) R.K.McGuire; "Seismic Structural Response Analysis, Incorporating Peak Response Regressions on Earthquake Magnitude and Distance", Research Report R74-51, Massachusetts Institute of Technology, Aug., 1974.

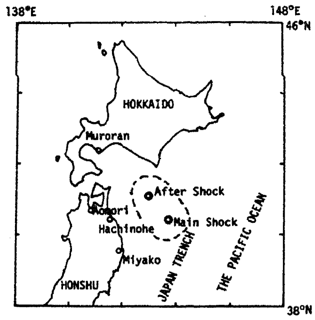

Fig.1. Locations of Epicenters and Observation Stations.

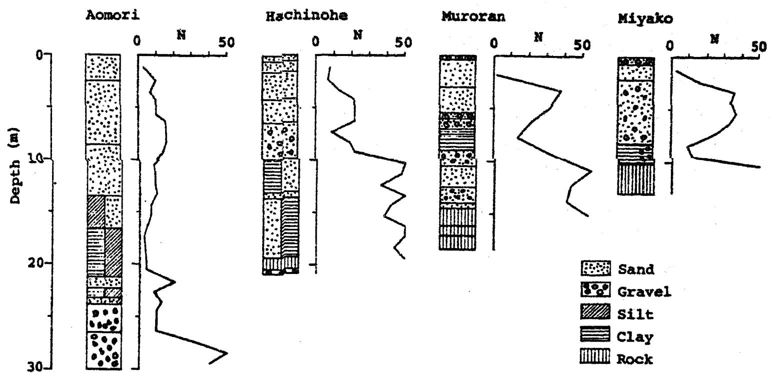

Fig.2. Boring Logs and N-Values.

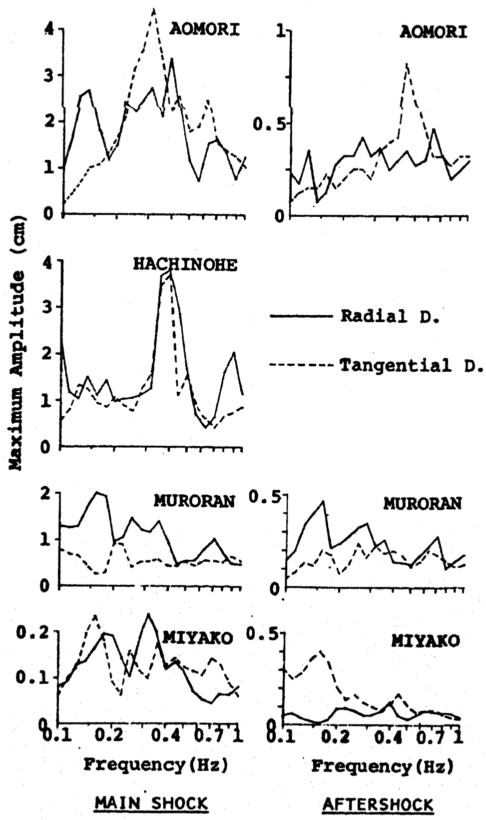

Fig.4. Maximum Amplitudes of Displacement Components with Different Frequency.

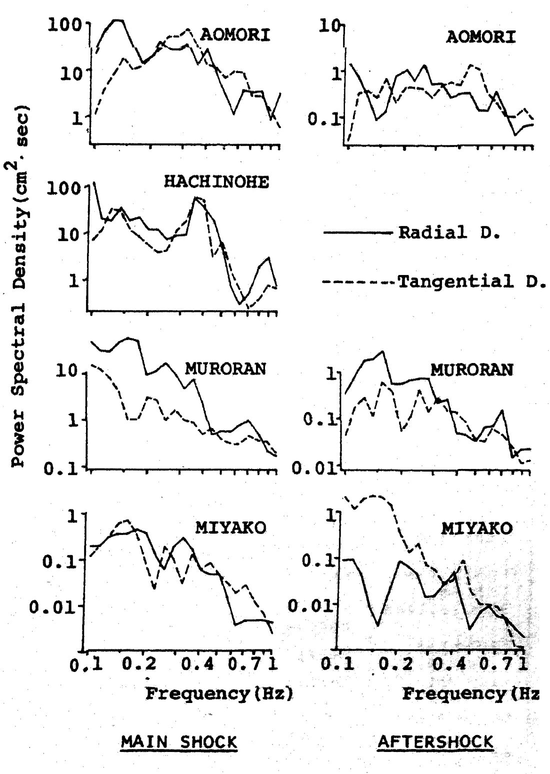

Fig.5. Power Spectral Densities for Calculated Displacements.

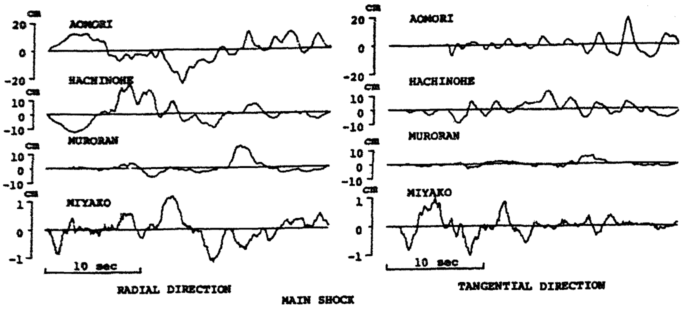

Fig.3. Calculated Displacement Curves.

Table 2. Ratios of r.m.s. Amplitudes during Aftershock and Main Shock.

Station	Component	Accel.	Vel.	Displ.
AOMORI	Radial	0.51	0.26	0.14
	Tan.	0.44	0.23	0.16
MURORAN	Radial	0.39	0.30	0.22
	Tan.	0.51	0.38	0.28
MIYAKO	Radial	0.76	0.67	0.47
	Tan.	0.51	0.79	1.76

Table 1. Maximum and r.m.s. Amplitudes.

Earthquake	Station Record No. Epicent.D.	Component	Acceleration (gal)		Velocity (kine)		Displacement (cm)	
			max.	σ	max.	σ	max.	σ
MAIN SHOCK	AOMORI S-235 243km	N-S	208.	44.3	37.6	10.5	18.7 (19.4)	4.52 (4.44)
Origin Time 9h49m, May 16,1968		E-W	177.	42.7	23.9	9.35	23.6 (12.6)	7.99 (4.42)
Epicenter 40.7°N 143.7°E		Radial	174.	42.7	25.4	9.43	23.9 (12.8)	8.17 (4.53)
Depth 0km		Tan.	211.	44.3	38.3	10.4	18.8 (19.5)	4.43 (4.36)
M=7.9	HACHINOHE S-252 188km	N-S	223.	40.8	32.5	7.79	12.4 (9.03)	4.16 (3.30)
		E-W	183.	45.1	39.3	9.01	20.4 (10.4)	7.26 (3.39)
		Radial	183.	45.2	39.6	9.11	21.0 (10.5)	7.49 (3.45)
		Tan.	221.	40.8	32.5	7.79	12.9 (8.97)	4.28 (3.32)
	MURORAN S-234 290km	N-S	199.	42.8	31.6	4.70	13.7 (8.47)	3.57 (2.34)
		E-W	133.	40.6	15.5	4.42	7.73 (5.73)	2.80 (2.13)
		Radial	190.	45.5	29.1	5.34	15.4 (9.31)	4.22 (2.84)
		Tan.	154.	37.5	16.6	3.58	5.72 (3.68)	1.74 (1.30)
	MIYAKO S-236 188km	N-S	111.	33.4	5.57	1.32	1.37 (1.16)	0.466 (0.376)
		E-W	94.3	27.5	3.83	1.09	1.41 (0.967)	0.417 (0.316)
		Radial	123.	28.1	4.09	1.13	1.21 (0.814)	0.442 (0.316)
		Tan.	115.	32.8	5.83	1.26	1.08 (0.987)	0.328 (0.322)
AFTERSHOCK	AOMORI S-264 218km	N-S	64.5	19.7	9.30	2.55	2.83 (2.06)	0.932 (0.769)
Origin Time 19h39m, May 16,1968		E-W	81.8	21.7	9.17	2.34	3.48 (2.27)	0.865 (0.574)
Epicenter 41.4°N 143.3°E		Radial	82.9	22.0	9.19	2.45	3.68 (2.40)	0.954 (0.638)
Depth 40km		Tan.	67.0	19.4	8.03	2.42	1.84 (1.97)	0.755 (0.688)
M=7.5	MURORAN S-241 218km	N-S	89.2	19.7	5.40	1.35	1.70 (1.07)	0.554 (0.343)
		E-W	73.9	17.2	5.06	1.62	2.31 (1.77)	0.873 (0.638)
		Radial	80.1	17.9	5.16	1.60	2.34 (1.66)	0.985 (0.629)
		Tan.	72.4	19.0	4.73	1.36	1.26 (1.06)	0.520 (0.366)
	MIYAKO S-271 226km	N-S	88.1	20.7	3.20	0.795	0.859 (0.717)	0.277 (0.211)
		E-W	73.6	17.4	3.23	0.914	2.71 (0.975)	1.13 (0.486)
		Radial	101.	21.2	3.06	0.752	0.626 (0.465)	0.188 (0.150)
		Tan.	73.0	16.8	3.88	0.995	2.90 (1.10)	1.30 (0.567)

The values in parentheses are the results for components with frequency greater than 0.1Hz.